A Benchmark Dataset for SSVEP-Based Brain–Computer Interfaces

Yijun Wang, *Member, IEEE*, Xiaogang Chen, Xiaorong Gao, *Member, IEEE*, and Shangkai Gao, *Fellow, IEEE*

Abstract—This paper presents a benchmark steady-state visual evoked potential (SSVEP) dataset acquired with a 40-target brain–computer interface (BCI) speller. The dataset consists of 64-channel Electroencephalogram (EEG) data from 35 healthy subjects (8 experienced and 27 naïve) while they performed a cue-guided target selecting task. The virtual keyboard of the speller was composed of 40 visual flickers, which were coded using a joint frequency and phase modulation (JFPM) approach. The stimulation frequencies ranged from 8 Hz to 15.8 Hz with an interval of 0.2 Hz. The phase difference between two adjacent frequencies was 0.5π. For each subject, the data included six blocks of 40 trials corresponding to all 40 flickers indicated by a visual cue in a random order. The stimulation duration in each trial was five seconds. The dataset can be used as a benchmark dataset to compare the methods for stimulus coding and target identification in SSVEP-based BCIs. Through offline simulation, the dataset can be used to design new system diagrams and evaluate their BCI performance without collecting any new data. The dataset also provides high-quality data for computational modeling of SSVEPs. The dataset is freely available from http://bci.med.tsinghua.edu.cn/download.html.

Index Terms—Brain–computer interface (BCI), electroencephalogram (EEG), joint frequency and phase modulation (JFPM), public data set, steady-state visual evoked potential (SSVEP).

I. Introduction

BRAIN–computer interfaces (BCIs) provide humans a new communication channel based on information coding and decoding with brain activities [1]–[3]. In recent years, electroencephalogram (EEG)-based BCIs have achieved rapid progress in performance, functionality, and practicality. Especially, the BCI performance has been substantially improved by the applications of advanced signal processing and machine

Y. Wang is with the State Key Laboratory on Integrated Optoelectronics, Institute of Semiconductors, Chinese Academy of Sciences, Beijing 100083, China (e-mail: wangyj@semi.ac.cn).

X. Chen is with the Institute of Biomedical Engineering, Chinese Academy of Medical Sciences and Peking Union Medical College, Tianjin 300192, China (e-mail: chenxg@bme.cams.cn).

X. Gao and S. Gao are with the Department of Biomedical Engineering, Tsinghua University, Beijing 100084, China (e-mail: gxrdea@tsinghua.edu.cn; gsk-dea@tsinghua.edu.cn).

learning algorithms. In the past decade, freely available BCI datasets played an important role in pushing forward the development of these algorithms. For example, the four international BCI Competitions [4]–[7] provided a large variety of BCI datasets from leading research groups. The datasets covered many BCI paradigms including slow cortical potentials (SCP), readiness potentials, event-related P300 potentials, and sensorimotor mu/beta rhythms. The resulting algorithms and techniques developed by researchers in a wide range of fields largely benefit the BCI community.

Recently, steady-state visual evoked potentials (SSVEPs) have been widely used in visual BCIs due to advantages of high information transfer rate (ITR) and little user training [8], [9]. Besides, the hybrid BCI approaches that combine SSVEP with other EEG signals (e.g., P300) have become more and more popular in recent studies [10]–[13]. However, to our knowledge, a benchmark dataset for SSVEP-based BCIs is still missing in the field. For detecting SSVEPs, researchers have developed many algorithms [14]–[17], which were evaluated with data collected by themselves. Due to the lack of a benchmark dataset, it is generally difficult to compare the performance of these algorithms. One of the major difficulties in collecting a benchmark dataset lies in the fact that there are a large variety of system diagrams in SSVEP-based BCIs (e.g., a binary selection system [18], and a 45-target speller [19]).

This study presents an open dataset for studying SSVEP-based BCIs. The dataset has the following features. 1) A large number of subjects (8 experienced and 27 naïve, 35 in total) were recorded. 2) A large number of stimulation frequencies (40, range: 8–15.8 Hz with an interval of 0.2 Hz) were included, and a 5-s stimulation for each frequency was repeated six times in recording. 3) Phase coding was also employed in stimulus coding. 4) Stimulus events (onsets and offsets) were accurately synchronized to EEG data. 5) 64-channel whole-head EEG data were recorded. These features make it possible to study algorithms for both SSVEP detection and stimulus coding with the dataset. Besides, through offline simulation, stimulus coding and target identification methods can be jointly considered towards the highest performance for an online BCI. High efficiency of such a benchmark dataset in the design of an SSVEP-based BCI has been preliminary shown by our recent studies in high-speed BCI spellers [20], [21].

The rest of this paper is organized as follows. Section II describes the experimental setups in data recording. Section III describes the data records and other related materials. Section IV presents basic approaches to analyze
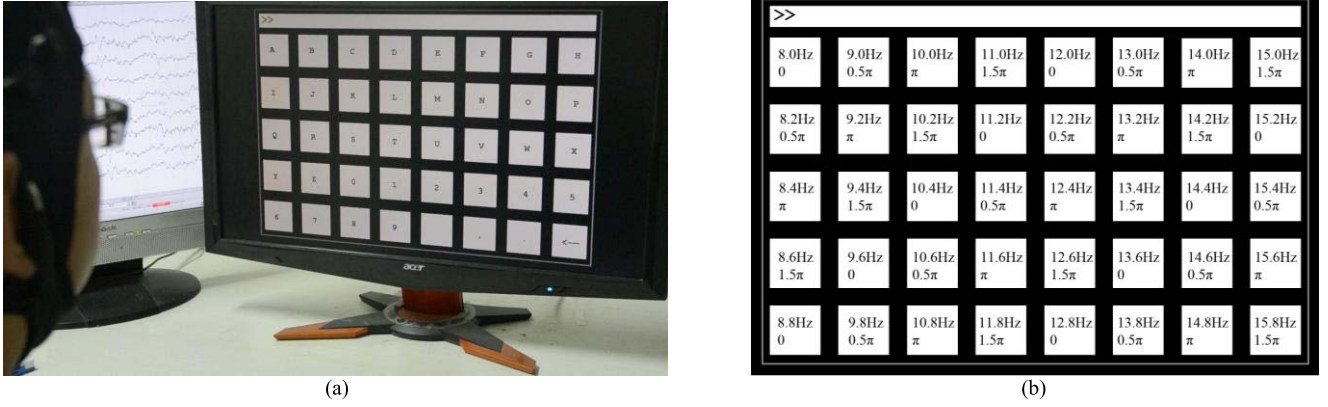
Fig. 1. (a) Stimulation interface of the 40-target BCI speller. (b) Frequency and phase values for all targets using the joint frequency and phase modulation method.

the data and shows two examples of how to use the dataset to study target detection and stimulus coding methods in SSVEP-based BCIs. Section V concludes and discusses the future work to improve the dataset.

II. METHODS

A. Participants

Thirty-five healthy subjects (17 females, aged 17–34 years, mean age: 22 years) with normal or corrected-to-normal vision participated in this study. Among all subjects, eight of them had experience of using the SSVEP-based BCI speller in our previous studies [20], [21]. Other 27 subjects were naïve to the SSVEP-based BCI. Each participant was asked to read and sign an informed consent form before the experiment. This study was approved by the Research Ethics Committee of Tsinghua University.

B. Stimulus Presentation

This study designed an offline BCI experiment using a 40-target BCI speller. Fig. 1(a) illustrates the 5×8 stimulus matrix of the speller, which contains 40 characters (26 English alphabets, 10 digits, and four symbols). The matrix was presented on a 23.6-in LCD monitor (Acer GD245 HQ, response time: 2 ms) with a resolution of 1920×1080 pixels at 60 Hz. The viewing distance to the screen was 70 cm. The sizes of stimulus and character were 140×140 ($3.2° \times 3.2°$) and 32×32 ($0.7° \times 0.7°$) pixels square, respectively. The size of the whole matrix area was 1510×1037 ($34° \times 24°$) pixels. The vertical and horizontal distances between two neighboring stimuli were both 50 pixels. The stimulus program was developed under MATLAB (MathWorks, Inc.) using the Psychophysics Toolbox Ver. 3 (PTB-3) [22].

The 40 characters were coded using a joint frequency and phase modulation (JFPM) approach [17]. The frequency and phase values for each character can be calculated as follows:

$$f\left(k_x, k_y\right) = f_0 + \Delta f \times [\left(k_y - 1\right) \times 5 + (k_x - 1)]$$
$$\varnothing\left(k_x, k_y\right) = \varnothing_0 + \Delta\varnothing \times [\left(k_y - 1\right) \times 5 + (k_x - 1)] \quad (1)$$

where k_x and k_y indicates the row and column index respectively. Here, f_0 and Δf was 8 Hz and 0.2 Hz respectively,

resulting in a frequency range of [8–15.8 Hz] for 40 characters. $\varnothing_0$ and $\Delta\varnothing$ were 0 and 0.5π respectively. Fig. 1(b) illustrates the frequency and phase values for each character.

This study adopted a sampled sinusoidal stimulation method [23], [19] to present visual flickers on the LCD monitor. At frequency f and phase $\varnothing$, the stimulus sequence $s(f, \varnothing, i)$ can be generated by modulating the luminance of the screen

$$s\left(f, \varnothing, i\right) = \frac{1}{2}\{1 + \sin\left[2\pi f \left(i/\text{RefreshRate}\right) + \varnothing\right]\} \quad (2)$$

where sin() generates a sine wave, and i indicates the frame index in the sequence. The refresh rate of the LCD monitor was 60 Hz. In the stimulus sequence, 0 represents dark and 1 represents the highest luminance.

C. Experimental Design

This study designed an offline BCI experiment using a cue-guided target selecting task. For each subject, the experiment included six blocks each containing 40 trials corresponding to all 40 characters indicated in a random order. Each trial started with a 0.5-s target cue (a red square at the target location, the same size as the stimulus). Subjects were asked to shift their gaze to the target as soon as possible. After the cue, all stimuli started to flicker on the screen concurrently for 5 s. Then, the screen was blank for 0.5 s before the next trial began. Each trial lasted 6 s in total. Subjects were instructed to avoid eye blinks during the 5-s stimulation duration. There was a rest for several minutes between two consecutive blocks.

D. Data Acquisition

This study used a Synamps2 EEG system (Neuroscan, Inc.) to record EEG data at a sampling rate of 1000 Hz. The usable bandwidth of the system was 0.15–200 Hz. Sixty-four electrodes according to an extended 10–20 system were used to record whole-head EEG. The reference electrode was placed at the vertex (Cz). Electrode impedances were kept below 10 kΩ during recording. Stimulus events generated by the stimulus program were recorded on an event channel synchronized to the EEG data. A notch filter at 50 Hz was applied to remove the power-line noise in recording. During the experiment,

subjects were seated in a comfortable chair in a dimly lit soundproof room.

E. Data Preprocessing

Data epochs were extracted from continuous EEG recordings according to stimulus onsets from the event channel. For each trial, six seconds (including 0.5 s before stimulus onset, 5 s for stimulation, and 0.5 s after stimulus offset) of data were extracted. Based on our previous finding that the upper-bound frequency of the SSVEP harmonics in this paradigm is around 90 Hz [19], all epochs were simply down-sampled to 250 Hz to reduce storage and computation costs. No digital filters were applied in data preprocessing.

F. Performance Evaluation

Classification accuracy and ITR are wildly used for evaluating BCI performance. ITR (in bits/min) can be estimated as follows [1]:

$$ ITR = \left(log_2 M + P log_2 P + (1-P) log_2 \left[\frac{1-P}{M-1} \right] \right) \times 60/T \tag{3} $$

where M is the number of classes, P is the accuracy of target identification, and T (seconds/selection) is the average time for a selection.

Both supervised and unsupervised algorithms have been developed for target identification in SSVEP-based BCIs. For supervised algorithms, a leave-one-out cross-validation (on six blocks) can be used to estimate classification accuracy and ITR. Note that, for the estimation of practical ITRs, the gaze shifting time (e.g., 2 s) should be added to T in the calculation. In practice, the gaze shifting time could vary across applications and subjects.

G. Simulation of Stimulation Phase

Because the stimulation signals and EEG data were accurately synchronized, the dataset can be used to simulate SSVEPs at any stimulation phase for the 40 frequencies. Note that, at the transition stage preceding the steady-state stage, amplitude and phase of the simulated data and the real data could differ slightly. New data epochs can be extracted by adding time shifts determined by given frequency and phase. For stimulation frequency f_k, the data epochs $\mathbf{X}$ can be first shifted circularly to the left with a time shift to generate SSVEPs with a zero initial phase

$$ \bar{X}(f_k, 0, n) = \mathbf{X} \left(f_k, \emptyset_k, n + \frac{(2\pi - \emptyset_k) \times f_s}{2\pi \times f_k} \right) \tag{4} $$

where n is the index of data sample, $\emptyset_k$ is the initial phase, and f_s is the sampling rate. To simulate a new phase value of $\bar{\emptyset}_k$, the zero-phase epochs can be shifted circularly with a time shift to generate new SSVEPs epochs

$$ \hat{X}(f_k, \bar{\emptyset}_k, n) = \bar{X} \left(f_k, 0, n + \frac{\bar{\emptyset}_k \times f_s}{2\pi \times f_k} \right). \tag{5} $$

III. DATA RECORDS

A. EEG Data

The dataset is freely available on http://bci.med.tsinghua.edu.cn/download.html. It contains 35 MATLAB MAT files corresponding to data from all subjects (approximately 3.3 GB in total). Data were stored as double-precision floating-point values in MATLAB. The files were named as subject indices (i.e., S01.mat, ..., S35.mat). For each file, the data loaded in MATLAB generate a 4-D matrix named "data" with dimensions of [64, 1500, 40, 6]. The four dimensions indicate "Electrode index", "Time points", "Target index", and "Block index", respectively. In terms of single trials, the data matrix consists of 240 trials (40 targets × 6 blocks) and each trial consists of 64 channels of 1500-point data. As described in the Data Preprocessing subsection, the data length of six seconds (i.e., $6 \times 250 = 1500$ time points) include 0.5 s before stimulus onset, 5 s for stimulation, and 0.5 s after stimulus offset. To keep all original information, the data epochs were directly extracted from the raw continuous data without any processing. A "Readme.txt" file explains the data structure and other task-related information.

B. Electrode Position

The electrode positions were saved in a "64-channels.loc" file, which included all channel locations in polar coordinates. Information for each electrode included four columns: "Electrode Index", "Degree", "Radius", and "Label". For example, information of the first electrode was as follows: ("1", "-17.926", "0.51499", and "FP1"), which indicated that the degree is -17.926 and the radius is 0.51499 for the first electrode (FP1). The electrode file can be imported into EEGLAB [24] for topographic analysis using the topoplot() function.

C. Subject Information

Information for all subjects was listed in a "Sub_info.txt" file. For each subject, there are five factors including "Subject Index", "Gender", "Age", "Handedness", and "Group". Subjects were divided into an "experienced" group (8 subjects, S01-S08) and a "naïve" group (27 subjects, S09-S35) according to their experience in SSVEP-based BCIs.

IV. TECHNICAL VALIDATIONS

A. Temporal Waveform, Amplitude Spectrum, and Signal-to-Noise Ratio (SNR) Analysis

To evaluate the signal quality of the dataset, this study analyzed temporal waveform, amplitude spectrum, and SNR of SSVEPs across all subjects. Fig. 2(a) shows the temporal waveform of averaged 15 Hz SSVEPs from the Oz electrode across all subjects. For each subject, the six trials of SSVEPs at 15 Hz were averaged first. To better observe the temporal characters of the SSVEPs, the data were band-pass filtered between 7 Hz and 70 Hz. The waveform is a near-sinusoidal signal at 15 Hz, which is time-locked to the stimulus onset
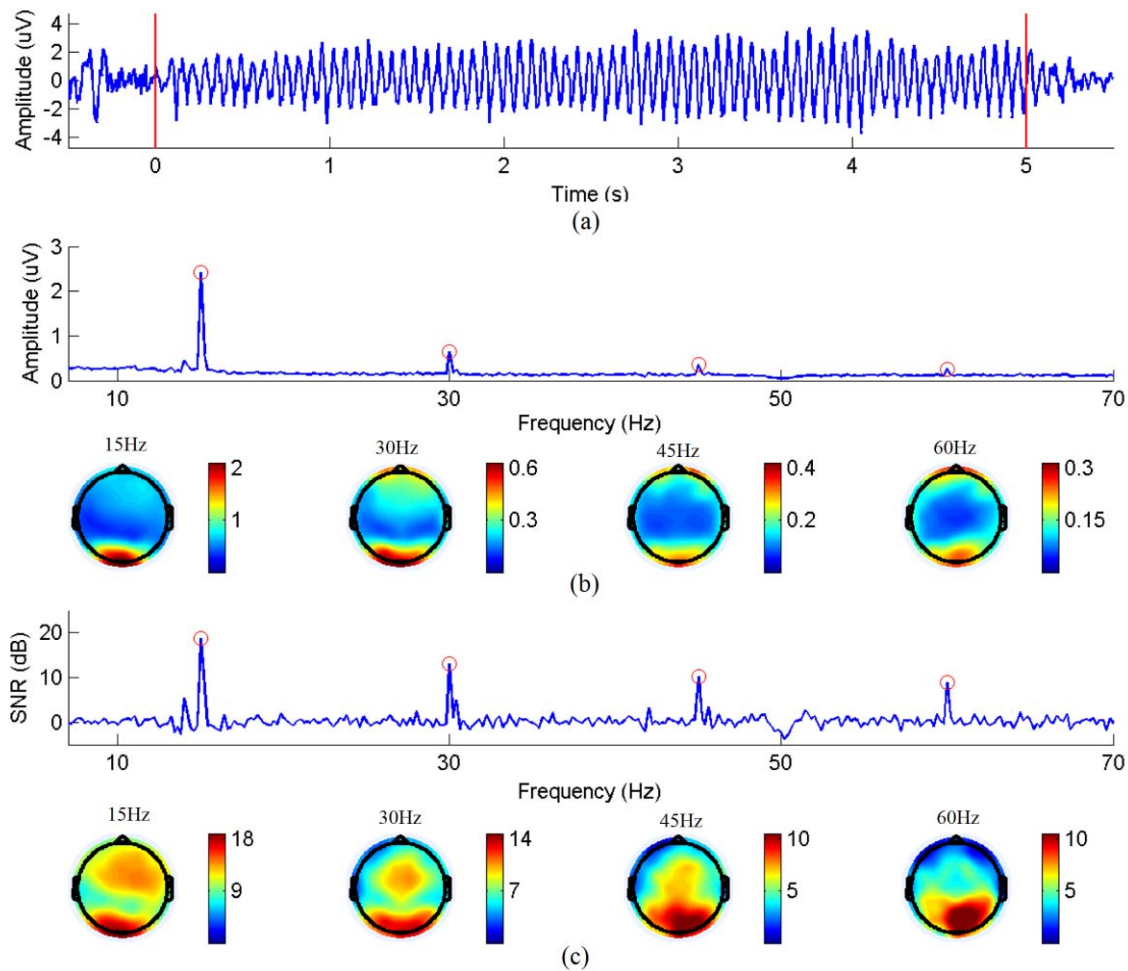
Fig. 2. (a) Average 15Hz SSVEP waveforms from the Oz electrode. Two lines at time 0 and 5 indicate the stimulus onset and offset respectively. The ERPs before time 0 were the brain's responses to the target cue. (b) Average amplitude spectrum of 15 Hz SSVEPs and the scalp maps at the fundamental, second, third, and fourth harmonic frequencies (i.e., 15 Hz, 30 Hz, 45 Hz, and 60 Hz). (c) Average SNR of 15 Hz SSVEPs and the scalp maps at the fundamental and harmonic frequencies. The red circles indicate the stimulation frequency and its harmonic frequencies.

with a delay around 130–140 ms [20]. The frequency and phase of the SSVEPs are stable over the 5-s stimulation time. Fig. 2(b) illustrates the amplitude spectrum of 15 Hz SSVEPs, which was estimated by averaging the amplitude spectra from six blocks and all subjects. Amplitude peaks can be observed at 15 Hz and its harmonic frequencies (i.e., 30 Hz, 45 Hz, 60 Hz). The amplitude of fundamental and harmonic components decreased sharply as the response frequency increased (fundamental: 2.41 uV, second harmonic: 0.64 uV, third harmonic: 0.35 uV, fourth harmonic: 0.25 uV). Fig. 2(c) shows the averaged SNR of SSVEPs at 15 Hz. This study defines SNR as the ratio of the amplitude at a given frequency f to the mean amplitude of signals within the 2 Hz neighboring frequency band $[f - 1\ f + 1]$. Compared with the amplitude spectrum, the SNRs decreased relatively slowly following the increase of response frequency (fundamental: 18.69 dB, second harmonic: 13.06 dB, third harmonic: 10.20 dB, fourth harmonic: 8.97 dB). This character suggests that the harmonic components provide useful information for detecting SSVEPs. Fig. 2(b) and (c) also illustrate the scalp topographies of amplitude and SNR of SSVEPs at 15 Hz and

its harmonic frequencies. In general, the occipital area shows the highest amplitude and SNR. Compared with the amplitude maps, the SNR maps show wider scalp distributions over the occipital and parietal areas. Some high frequency activities, which might be caused by eye movement artifacts, can be observed at the prefrontal area only in the amplitude maps (at 30 Hz, 45 Hz, and 60 Hz).

The temporal, frequency, and spatial features of the 15 Hz SSVEP described above are consistent across all stimulation frequencies. Fig. 3 illustrates the amplitude spectrum and SNR images as functions of stimulation frequency and response frequency [25]. In addition to the averaging process described above, the amplitude spectrum and SNR were also averaged across nine electrodes over the occipital and parietal areas (Pz, PO5, PO3, POz, PO4, PO6, O1, Oz, and O2) to remove the background EEG activities. For all 40 stimulation frequencies, the fundamental, second, third, and fourth harmonics can be observed in the amplitude spectrum image, while more harmonics (up to the eighth harmonic) can be clearly identified in the SNR image with an upper-bound frequency around 90 Hz. These results show very robust and reliable frequency features
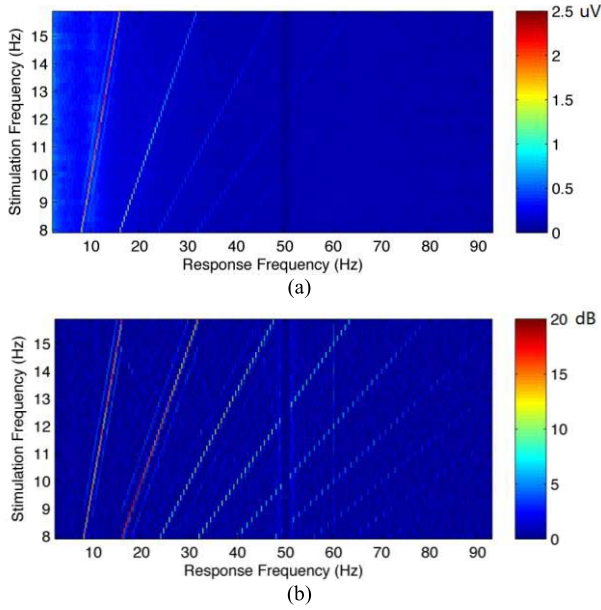
Fig. 3. (a) Amplitude spectra of SSVEPs for all 40 stimulation frequencies (8 Hz to 15.8 Hz with an interval of 0.2 Hz) as a function of stimulation frequency and response frequency. (b) SNRs for all 40 stimulation frequencies. The amplitude and SNR drops at 50 Hz were caused by the notch filter.
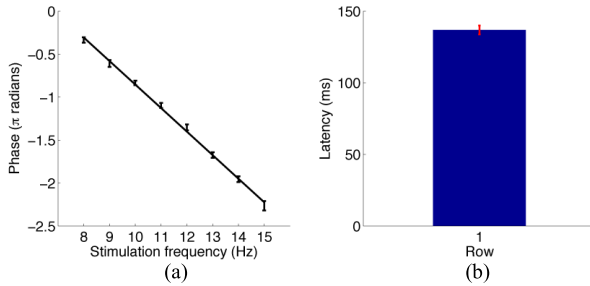

Fig. 4. (a) Average phases of SSVEPs (in π radians) across all subjects. The frequencies from 8 Hz to 15 Hz with an interval of 1 Hz (i.e., the first row of the stimulation matrix) were used in the estimation. A linear model was used to fit the phase data. (b) Estimated visual latency across all subjects. The error bars indicate standard errors.

for the fundamental and harmonic SSVEP components in the dataset.

B. Estimation of Phase and Visual Latency

The visual latency between the stimulus and the SSVEP response plays an important role in SSVEP detection. An accurate estimation of the visual delay ensures that the extracted data epochs only contain SSVEP responses to the stimulation. The visual latency can be obtained by measuring phase as a function of stimulation frequency and estimating the slope of the phase curve [26]. Fig. 4(a) shows the average phases of SSVEPs at eight integer frequencies (from 8 to 15 Hz) across all subjects. SSVEPs from the Oz electrode were used in the estimation. A linear model fits the phase data well, which suggests that visual latency can be considered as a constant within the frequency range used in this study. The mean visual latency estimated from the linear model
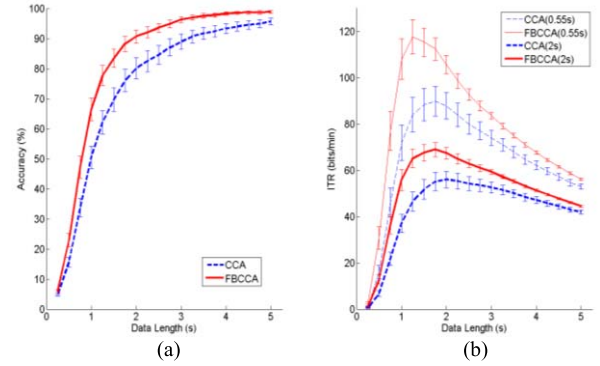

Fig. 5. (a)Classification accuracy for the CCA and FBCCA methods with different data lengths from 0.25 s to 5 s with a step of 0.25 s. (b) ITRs corresponding to the accuracy. Two durations (0.55 s and 2 s) were used as gaze shifting time in the calculation of ITR. The error bars indicate standard errors.

is 136.91±18.4 ms [Fig. 4(b)], which is consistent to our previous studies [20], [21]. These results prove the stability of visual latency across stimulation frequencies in the dataset. As a result, in data analysis, a time delay of $\sim$ 140 ms should be added in the extraction of SSVEP epochs.

C. Evaluating the Filter Bank Canonical Correlation Analysis (FBCCA) Method

The canonical correlation analysis (CCA) method has been widely used in frequency detection of SSVEPs [15]. To better integrate information from the fundamental and harmonic components for SSVEP detection, we recently proposed an FBCCA method in [20] and demonstrated its superiority over the standard CCA method. Here we adopted the FBCCA method to classify the 40-class SSVEPs for all subjects in the dataset. Data from nine electrodes (Pz, PO5, PO3, POz, PO4, PO6, O1, Oz, and O2) were used as the input to the filter bank analysis. The same parameters from [20] were used in feature extraction and classification. More details of the FBCCA method can be found in [20]. Fig. 5(a) and (b) show the classification accuracy and ITR respectively with different data lengths of SSVEPs. Results from the CCA method were also included for comparison. For both accuracy and ITR, the FBCCA method significantly outperformed the CCA method. The classification accuracy increased as the data length increased. To estimate both practical and theoretical ITRs, this study used two different durations (i.e., 2 s and 0.55 s) of gaze shifting time in the calculation of ITR. With a 2 s duration [10], [11], the ITRs show peak values of 68.99 bits/min (data length: 1.75 s) for the FBCCA method and 56.03 bits/min (data length: 2 s) for the CCA method. With a 0.55 s duration [20], the peak ITRs increased to 117.75 bits/min (data length: 1.25 s) and 89.89 bits/min (data length: 1.75 s) for FBCCA and CCA, respectively. This example suggests that the dataset can be used to evaluate the performance of new methods for SSVEP detection.

D. Evaluating the JFPM Approach

Advanced stimulus coding approaches are highly efficient for improving the performance of SSVEP-based BCIs [3].
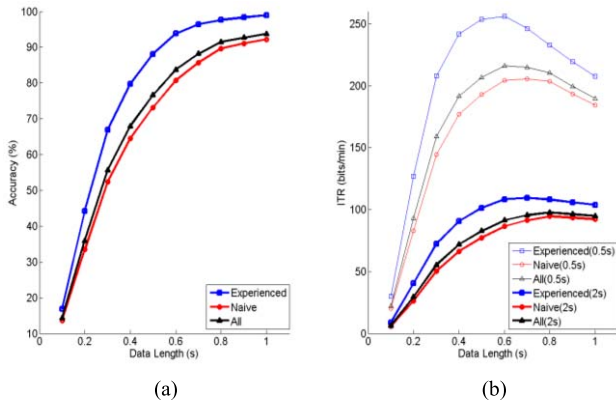
Fig. 6. (a) Classification accuracy for the JFPM method with different data lengths from 0.1 s to 1 s with a step of 0.1 s. Results for the experienced, naïve, and all subjects were calculated separately. (b) ITRs corresponding to the accuracy. The phase interval value (0.35π) and other parameters in feature extraction and classification were the same as [21]. Two durations (0.5 s and 2 s) were used as gaze shifting time in the calculation of ITR.

To test the usability of the dataset in studying stimulus coding approaches, this study adopted the JFPM approach [21] to simulate an offline BCI speller. In the JFMP approach, in addition to frequency coding, the phase difference between two adjacent frequencies can facilitate the classification based on a template matching method. According to [21], the phase interval value was set to 0.35π. To simulate new stimulation phases, data epochs were extracted according to (4) and (5). Fig. 6 shows the classification accuracy and ITR for three subject groups (i.e., 8 experienced, 27 naïve, and all 35 subjects). With a 2 s gaze shifting time, the peak ITR for the experienced subjects was 109.50 bits/min (data length: 0.7 s). The naïve subjects had a lower peak ITR of 94.55 bits/min (data length: 0.8 s). The peak ITR across all subjects was 97.64 bits/min (data length: 0.8 s). When using a 0.5 s gaze shifting time [21], the peak ITR for the experienced group increased to 255.98 bits/min (data length: 0.6 s), which was comparable to the results reported in [21]. In real practice, an average ITR around 100 bits/min can satisfy the requirement of a high-speed BCI for communication and control. This example shows the feasibility of using the dataset to develop new stimulus coding approaches for SSVEP-based BCIs.

V. CONCLUSION AND DISCUSSIONS

This study presents a benchmark dataset for studying SSVEP-based BCIs. The dataset is an extended version of the data published in our recent studies on high-speed BCI spellers [20], [21]. Distinct SSVEP features in temporal, frequency, and spatial domains prove the high quality of data across all subjects. The two examples on the FBCCA and JFPM approaches further demonstrate high efficiency of the dataset for evaluating methods in SSVEP detection and stimulus coding, respectively.

This study used different durations of gaze shifting time (long: 2 s, short: 0.55 s for the FBCCA method in Fig. 5 and 0.5 s for the JFPM method in Fig. 6) to estimate the practical and theoretical ITRs of the BCI speller. In real practice of spelling, a 2 s duration is sufficient for experienced users

to locate and switch gaze to a target [10], [11]. However, a 0.5 s duration, which is close to the speed limit of gaze control [21], might not be sufficient for target switching in free spelling. Assuming the participants could achieve this speed in target switching, the resulting ITR would be comparable to the theoretical ITRs reported above. Further investigation with a large amount of subjects is required to estimate the realistic ITR in free spelling.

In addition to the technical validations presented in this study, the dataset can be further analyzed in different ways. On one hand, the dataset can be used to design system diagrams towards different applications. The optimization of parameters is very important for the design and implementation of a practical BCI system [8]. For example, to implement a BCI for two-dimensional movement control, eight frequencies can be selected from the 40 frequencies towards the highest BCI performance. The JFPM approach also requires optimization to find the best phase interval value. Besides, the number of electrodes and electrode locations can be optimized using the 64-channel dataset. On the other hand, the dataset can be used to develop computational models for SSVEPs. The high SNR of SSVEPs from the dataset could be helpful for exploring the intrinsic properties of SSVEP harmonics. For example, the way to characterize the phases of the fundamental and harmonic SSVEP components still remains unknown.

The BCI speller described in this study is a gaze-dependent system, which requires accurate gaze control. For locked-in patients who lose their ability in oculomotor control, only gaze-independent BCIs [27] are applicable. Some open data sets of gaze-independent BCIs can be found at [28].

In future work, the dataset can be improved in the following directions. First, data from online BCI experiments will be included. A direct comparison between online and offline experiments can help to better predict the online BCI performance through offline simulation. Second, data from more subjects will be added to improve the cross-subject analysis such as the generalized templates-based approach for SSVEP detection [29]. Third, data records from the same group of subjects on different days will be provided for developing the session-to-session transfer approach [30], which can facilitate system calibration of an online BCI.

REFERENCES

[1] J. R. Wolpaw, N. Birbaumer, D. J. McFarland, G. Pfurtscheller, and T. M. Vaughan, "Brain–computer interfaces for communication and control," *Clin. Neurophysiol.*, vol. 113, no. 6, pp. 767–791, 2002.

[2] M. A. Lebedev and M. A. L. Nicolelis, "Brain–machine interfaces: Past, present and future," *Trends Neurosci.*, vol. 29, no. 9, pp. 536–546, 2006.

[3] S. Gao, Y. Wang, X. Gao, and B. Hong, "Visual and auditory brain–computer interfaces," *IEEE Trans. Biomed. Eng.*, vol. 61, no. 5, pp. 1436–1447, May 2014.

[4] P. Sajda, A. Gerson, K. R. Müller, B. Blankertz, and L. Parra, "A data analysis competition to evaluate machine learning algorithms for use in brain-computer interfaces," *IEEE Trans. Neural Syst. Rehabil. Eng.*, vol. 11, no. 2, pp. 184–185, Jun. 2003.

[5] B. Blankertz *et al.*, "The BCI competition 2003: Progress and perspectives in detection and discrimination of EEG single trials," *IEEE Trans. Biomed. Eng.*, vol. 51, no. 6, pp. 1044–1051, Jun. 2004.

[6] B. Blankertz *et al.*, "The BCI competition. III: Validating alternative approaches to actual BCI problems," *IEEE Trans. Neural Syst. Rehabil. Eng.*, vol. 14, no. 2, pp. 153–159, Jun. 2006.

[7] M. Tangermann *et al.*, "Review of the BCI competition IV," *Front. Neurosci.*, vol. 6, p. 55, Jul. 2012.

[8] Y. Wang, X. Gao, B. Hong, C. Jia, and S. Gao, "Brain–computer interfaces based on visual evoked potentials," *IEEE Eng. Med. Biol. Mag.*, vol. 27, no. 5, pp. 64–71, Sep./Oct. 2008.

[9] F. B. Vialatte, M. Maurice, J. Dauwels, and A. Cichocki, "Steady-state visually evoked potentials: Focus on essential paradigms and future perspectives," *Prog. Neurobiol.*, vol. 90, no. 4, pp. 418–438, 2010.

[10] M. Xu *et al.*, "A visual parallel-BCI speller based on the time-frequency coding strategy," *J. Neural Eng.*, vol. 11, no. 2, p. 026014, 2014.

[11] E. Yin, Z. Zhou, J. Jiang, F. Chen, Y. Liu, and D. Hu, "A novel hybrid BCI speller based on the incorporation of SSVEP into the P300 paradigm," *J. Neural Eng.*, vol. 10, no. 2, p. 026012, 2013.

[12] M. Wang *et al.*, "A new hybrid BCI paradigm based on P300 and SSVEP," *J. Neurosci. Methods*, vol. 244, pp. 16–25, Apr. 2015.

[13] Y. Li *et al.*, "Multimodal BCIs: Target detection, multidimensional control, and awareness evaluation in patients with disorder of consciousness," *Proc. IEEE*, vol. 104, no. 2, pp. 332–352, Feb. 2016.

[14] O. Friman, I. Volosyak, and A. Graser, "Multiple channel detection of steady-state visual evoked potentials for brain-computer interfaces," *IEEE Trans. Biomed. Eng.*, vol. 54, no. 4, pp. 742–750, Apr. 2007.

[15] G. Bin, X. Gao, Z. Yan, B. Hong, and S. Gao, "An online multi-channel SSVEP-based brain-computer interface using a canonical correlation analysis method," *J. Neural Eng.*, vol. 6, no. 4, p. 046002, 2009.

[16] Y. Zhang, G. Zhou, J. Jin, X. Wang, and A. Cichocki, "Frequency recognition in SSVEP-based BCI using multiset canonical correlation analysis," *Int. J. Neural Syst.*, vol. 24, no. 4, pp. 1450013-1–1450013-14, 2014.

[17] Y. Zhang, P. Xu, K. Cheng, and D. Yao, "Multivariate synchronization index for frequency recognition of SSVEP-based brain-computer interface," *J. Neurosci. Methods*, vol. 221, pp. 32–40, 2014.

[18] E. C. Lalor *et al.*, "Steady-state VEP-based brain-computer interface control in an immersive 3D gaming environment," *EURASIP J. Appl. Signal Process.*, vol. 19, pp. 3156–3164, Jan. 2005.

[19] X. Chen, Z. Chen, S. Gao, and X. Gao, "A high-ITR SSVEP based BCI speller," *Brain-Comput. Interfaces*, vol. 1, nos. 3–4, pp. 181–191, 2014.

[20] X. Chen, Y. Wang, S. Gao, T. P. Jung, and X. Gao, "Filter bank canonical correlation analysis for implementing a high-speed SSVEP-based brain-computer interface," *J. Neural Eng.*, vol. 12, no. 4, p. 046008, 2015.

[21] X. Chen, Y. Wang, M. Nakanishi, X. Gao, T. P. Jung, and S. Gao, "High-speed spelling with a noninvasive brain-computer interface," *Proc. Nat. Acad. Sci. USA*, vol. 112, no. 44, pp. E6058–E6067, 2015.

[22] D. H. Brainard, "The psychophysics toolbox," *Spatial Vis.*, vol. 10, no. 4, pp. 433–436, 1997.

[23] N. V. Manyakov, N. Chumerin, A. Robben, A. Combaz, M. van Vliet, and M. M. van Hulle, "Sampled sinusoidal stimulation profile and multichannel fuzzy logic classification for monitor-based phase-coded SSVEP brain-computer interfacing," *J. Neural Eng.*, vol. 10, no. 3, p. 036011, 2013.

[24] A. Delorme and S. Makeig, "EEGLAB: An open source toolbox for analysis of single-trial EEG dynamics including independent component analysis," *J. Neurosci. Methods*, vol. 134, no. 1, pp. 9–21, Mar. 2004.

[25] C. S. Herrmann, "Human EEG responses to 1-100 Hz flicker: Resonance phenomena in visual cortex and their potential correlation to cognitive phenomena," *Exp. Brain Res.*, vol. 137, nos. 3–4, pp. 346–353, 2001.

[26] F. D. Russo and D. Spinelli, "Electrophysiological evidnece for an early attentional mechanism in visual processing in humans," *Vis. Res.*, vol. 39, no. 18, pp. 2975–2985, 1999.

[27] A. Riccio, D. Mattia, L. Simione, M. Olivetti, and F. Cincotti, "Eye-gaze independent EEG-based brain-computer interfaces for communication," *J. Neural Eng.*, vol. 9, no. 4, p. 045001, 2012.

[28] [Online]. Available: http://bnci-horizon-2020.eu/database/data-sets

[29] P. Yuan, X. Chen, Y. Wang, X. Gao, and S. Gao, "Enhancing performances of SSVEP-based brain-computer interfaces via exploiting inter-subject information," *J. Neural Eng.*, vol. 12, no. 4, p. 046006, 2015.

[30] M. Krauledat, M. Tangermann, B. Blankertz, and K. R. Müller, "Towards zero training for brain-computer interfacing," *PLoS One*, vol. 3, no. 8, p. e2967, 2008.

Yijun Wang (M'11) received his B.E. and Ph.D. degrees in biomedical engineering from Tsinghua University, Beijing, China, in 2001 and 2007, respectively.

From 2008 to 2015, he was first a postdoctoral researcher and later an assistant project scientist at the Swartz Center for Computational Neuroscience, University of California San Diego. Since 2015, he has been a research fellow with the Institute of Semiconductors, Chinese Academy of Sciences. His research interests include brain–computer interface, biomedical signal processing, and machine learning.

Xiaogang Chen received the B.E. degree in biomedical engineering from Xianning College, Xianning, China, in 2008, the M.E. degree in biomedical engineering from Hebei University of Technology, Tianjin, China, in 2011, and the Ph.D. degree in biomedical engineering from Tsinghua University, Beijing, China, in 2015.

He is currently working as Assistant Research Fellow in Institute of Biomedical Engineering, Chinese Academy of Medical Sciences. His research interests include brain–computer interface and biomedical signal processing.

Xiaorong Gao (M'04) received the B.S. degree in biomedical engineering from Zhejiang University, Zhejiang, China, in 1986, the M.S. degree in biomedical engineering from Peking Union Medical College, Beijing, China, in 1989, and the Ph.D. degree in biomedical engineering from Tsinghua University, Beijing, China, in 1992.

He is currently a Professor of the Department of Biomedical Engineering, Tsinghua University. His current research interests are biomedical signal processing and medical instrumentation, especially the study of brain–computer interface.

Shangkai Gao (SM'94–F'07) graduated from the Department of Electrical Engineering of Tsinghua University, Beijing, China, in 1970, and received the M.E. degree of biomedical engineering in 1982 in same department of Tsinghua University.

She is now a Professor of the Department of Biomedical Engineering in Tsinghua University. Her research interests include neural engineering and medical imaging, especially the study of brain–computer interface. She is now on the Editorial Board Member of the Journal of Neural Engineering and Physiological Measurement.

Prof. Gao is a Fellow of American Institute for Medical and Biological Engineering (AIMBE). She is now on the Editorial Board Member of the IEEE Transactions on Biomedical Engineering, as well as the Senior Editor of IEEE Transactions on Neural System and Rehabilitation Engineering.